

BRNO UNIVERSITY OF TECHNOLOGY  
VYSOKÉ UČENÍ TECHNICKÉ V BRNĚ

FACULTY OF ELECTRICAL ENGINEERING AND COMMUNICATION  
DEPARTMENT OF BIOMEDICAL ENGINEERING

FAKULTA ELEKTROTECHNIKY A KOMUNIKAČNÍCH TECHNOLOGIÍ  
ÚSTAV BIOMEDICÍNSKÉHO INŽENÝRSTVÍ

MODELLING OF THE HUMAN RESPIRATORY  
SYSTEM FOR CLINICALLY RELEVANT  
APPLICATIONS

MODELOVÁNÍ RESPIRAČNÍHO SYSTÉMU ČLOVĚKA PRO  
KLINICKY RELEVANTNÍ APLIKACE

SHORTENED PHD THESIS  
ZKRÁCENÁ VERZE DISERTAČNÍ PRÁCE

AUTHOR  
AUTOR PRÁCE

Ing. RICHARD PAŠTĚKA, MSc.

ACADEMIC ADVISOR  
ŠKOLITEL

doc. Ing. RADIM KOLÁŘ, Ph.D.

## **KEYWORDS**

human respiratory system modelling, lung simulation, breathing simulation, patient-ventilator interactions testing, aerosolised drug delivery

## **KLÍČOVÁ SLOVA**

modelování lidského dýchacího systému, simulace plic, simulace dýchání, testování interakcí mezi pacientem a ventilátorem, aerosolové podávání léčiv

## **PLACEMENT LOCATION**

library VUT

# Contents

|  |           |
|--|-----------|
| <b>Introduction</b>  | <b>4</b>  |
| <b>Aim of the thesis</b>   | <b>7</b>  |
| <b>1 Breathing simulation using polymer and organic human lung equivalents</b> | <b>8</b>  |
| 1.1 Introduction . . . . .   | 9         |
| 1.2 Materials & Methods . . . . .  | 9         |
| 1.3 Results . . . . .  | 10        |
| 1.4 Discussion . . . . .   | 13        |
| 1.5 Conclusion . . . . .   | 13        |
| <b>2 Patient-ventilator interaction testing</b>                                | <b>14</b> |
| 2.1 Introduction . . . . .   | 15        |
| 2.2 Materials & Methods . . . . .  | 15        |
| 2.3 Results . . . . .  | 16        |
| 2.4 Discussion . . . . .   | 19        |
| 2.5 Conclusion . . . . .   | 19        |
| <b>3 Experimental evaluation of dry powder inhalers</b>                        | <b>20</b> |
| 3.1 Introduction . . . . .   | 21        |
| 3.2 Materials and Methods . . . . .  | 21        |
| 3.3 Results and Discussion . . . . .   | 23        |
| 3.4 Summary and Conclusion . . . . .   | 26        |
| <b>Further directions &amp; future work</b>                                    | <b>27</b> |
| <b>Conclusion</b>  | <b>28</b> |
| <b>Curriculum Vitae</b>  | <b>33</b> |
| <b>Abstract</b>  | <b>36</b> |

# Introduction

The epidemiological transition is a term referring to a complex and dynamic process of the shift from acute infectious diseases to chronic non-communicable diseases [1], [2]. This transition has already largely occurred in developed high-income countries, where non-communicable diseases accounted for up to 85% of deaths in 2019 [3]. A rapid epidemiological transition can be observed in many middle-income countries as well [4]. In low-income countries, non-communicable diseases were responsible for more than half of all deaths and their fraction is predicted to further increase with modernisation [1]–[3]. Leading causes are diseases of the circulatory system, respiratory system, and cancer [3].

Most common respiratory diseases include chronic obstructive pulmonary disease (COPD), asthma, allergic diseases, occupational lung diseases, and pulmonary hypertension [5]. Risk factors such as smoking (in both active and passive form), occupational exposure to dust, fumes and chemicals, and air pollution in general, are among the reasons why the number of patients troubled by respiratory diseases continues to grow [3], [5]. Both asthma and COPD significantly affect a person’s ability to breathe and can be effectively treated at the primary care level with aerosol therapy [6]. According to the Global Asthma Network, up to 339 million people may be affected by asthma worldwide [7]. Furthermore 65 million people globally suffer from mild to severe COPD [8], [9]. Note that the most recently available statistics considered here do not include the effects of the COVID-19 pandemic. According to the estimations, respiratory coronavirus infectious disease, COVID-19, will be among the leading causes of death in 2020 and beyond, increasing the total toll of deaths significantly [3], [10].

Severe cases of respiratory diseases like COPD or COVID-19, can lead to respiratory failure [11]. Respiratory failure is a serious condition in which the respiratory system fails to maintain adequate gas exchange due to a failure of the lung (gas-exchanging organ) and/or the pump that ventilates the lungs [12]. Affected patients require mechanical ventilation to ensure oxygenation and carbon dioxide clearance [11]. During mechanical ventilation disparity between flow, pressure or volume demands of the patient and the assistance delivered by the mechanical ventilator leads to patient-ventilator asynchrony [13]. These asynchronies are linked with negative physical and mental outcomes such as higher mortality, excessive load on respiratory muscles, lung injury and prolonged ICU stay [13], [14]. For the reasons described above the testing and minimising of patient-ventilator interactions is a direction currently pursued and explored further in this thesis.

Chronic respiratory diseases are not curable and affect the lungs and airways [15]. These diseases can cause airflow limitation due to airway obstruction, an

abnormal inflammatory response of the lungs and other severe problems leading to breathing difficulties [15]. Various forms of treatment that help dilate major airways and increase patients' quality of life are well established [15]. Aerosol therapy is a treatment of choice due to easy drug delivery options, sustained localised action and the possibility of home therapy. The number of drugs delivered in the form of aerosols increases every year because of advancements in aerosol manufacturing and easy-to-use personal inhalation devices [16]. This trend is reflected in growing total worldwide sales of inhalation products [17]. Inhalation therapy devices can be categorised into four main types, including nebulisers, pressurised-metered dose inhalers (pMDI), soft mist inhalers (SMI), and dry powder inhalers (DPI) [18]. Such devices are being continuously developed, evaluated and tested under various conditions. For these reasons, the testing of DPIs is one of the key research topics explored in this thesis.

The statistics regarding respiratory disease covered here might provide a rather negative perspective on the trajectory of human pulmonary health. However, the increasing incidence of respiratory diseases is driving major scientific advances in the area of respiratory research. Various models of the human respiratory system are being developed to increase knowledge and to allow for studies of specific research questions. The common denominator is the effort of the researchers to provide the best possible treatment options for the patients.

Based on the experimental setup, the models used in respiratory research can be divided into four main categories: (1) *in vivo* (2) *in vitro* (3) *in silico* and (4) *ex vivo*. The use of models in respiratory research and the range of their possible applications is growing. *In vivo* based studies are testing various effects on whole, living organisms such as small animals (e.g. guinea pigs, rats, mice) [19], large animals (e.g. rabbits, pigs, non-human primates) [20] or humans. Animal experimentation has a prominent role in many scientific advancements but presents a challenging ethical dilemma of causing pain and suffering to the animal [21]. By complying with ethical guidelines and good scientific practices the animal welfare and human science principles can be upheld [21]. All modern research endeavours should comply with the principles of 3Rs that were proposed by Russell and Burch [22] in 1959. Namely [23]:

- "a *replacement* of animals in research, which results from an active development of alternatives;"
- "a *reduction* in the number of animals used in experiments;"
- "a *refinement* of laboratory and field techniques to reduce invasiveness and/or to increase the values of the results."

Subsequently, increasing efforts are being invested in the development and validation of alternatives to animal experimentation. These efforts have been instigated by legislative powers like the EU directive on the protection of animals used for

scientific purposes (2010/63/EU) and by the growing involvement of the general public [24]. The following paragraphs provide an overview of experimental setups that can be developed in compliance with 3Rs and hence provide alternatives to animal experimentation.

In vitro models can use isolated living components of organisms such as cells or biological molecules for experiments. However, animals and humans are not directly involved, except as donors of biological material [25]. In vitro studies are conducted in a laboratory vessel or elsewhere outside the living body. The latest in vitro models in the field of respiratory research are based on organ-on-a-chip, and microfluidic technologies [26]. Prominent examples include modelling and diagnosis of chronic respiratory diseases [27], toxicity assessment of various compounds [28] and development of novel drugs [29].

The in silico models (referring to the silicon used for semiconductor computer chips) are utilised to create computer representation of their in vivo counterparts (e.g., organs, systems and processes) [30]. Two breakthroughs facilitating rapid development in the area of in silico based respiratory models can be identified in recent years. The first impulse was the introduction of the respiratory tract model for radiological protection by the International Commission on Radiological Protection (ICRP) [31]. The second catalyst was the advancement of computational fluid-particle dynamics (CFPD) methods [32]. These methods offer a possibility to predict airflow and to localise aerosol particle deposition in the human respiratory tract [33].

The ex vivo models, also called in vitro tissue-based models, include procedures with living functional tissues or organs isolated from an organism and sustained outside the organism in an artificial environment under highly controlled conditions [34]. The ex vivo models allow for tests and measurements that would be difficult to conduct in a living subject under controlled conditions at all times [35]. They provide a valuable resource for translational medicine and are especially suitable for studying the mechanisms of lung injury, lung deposition of inhaled therapeutics on a regional level, and toxicity tests [19].

Original research presented in this thesis introduces and utilises a model of the human respiratory system xPULM™, that incorporates aspects of in vitro, in silico and ex vivo modelling approaches.

The use of models in respiratory research and the range of their possible applications is growing. For the context of this work the key applications include breathing and lung simulation [36], education and training of students/health professionals [37], testing of mechanical ventilators [38], and aerosolised drug delivery [39].

# Aim of the thesis

This thesis aims to establish a physical model of the human respiratory system (xPULM™) that represents an innovative approach to respiratory system behaviour modelling. To reach this aim, three clinically relevant applications were researched, namely (i) breathing simulation, (ii) patient-ventilator interaction testing and (iii) aerosolised drug delivery. The goals of the thesis consider the available instrumentation at the University of Applied Sciences Technikum Wien. This thesis has been developed as a part of continuous cooperation between the University of Applied Sciences Technikum Wien and the Brno University of Technology. Further cooperation partners include the University of Trás-os-Montes E Alto Douro and the hospital Centro Hospitalar De Trás-Os-Montes E Alto Douro whose engagement allowed for the acquisition of CT examinations from a retrospective clinical trial.

The goals of the thesis are to:

1. Determine the capability of the xPULM™ to reproducibly simulate human breathing patterns. The breathing simulation should be evaluated for a variety of breathing frequencies and tidal volumes while using different lung equivalents (e.g. polymer-based bags, lungs obtained from animals). Modify hardware and software components to advance the model towards anatomically and physiologically realistic breathing simulation.
2. Obtain information from a retrospective clinical trial focusing on realistic human upper airway geometry. Manufacture a physical model of the human upper respiratory tract and implement it into the existing measurement setup. The model should approximate anatomical structures (oral cavity, the pharyngeal region and the first centimetres after the larynx) of a healthy human.
3. Develop, implement and test a measurement setup allowing for simulation of a patient undergoing mechanical ventilation. Determine the undesired interactions occurring between the mechanical ventilator and the simulated patient. Discuss comparability of results to situations occurring in clinical practice.
4. Develop, implement and test a measurement setup allowing for experimental evaluation of dry powder inhalers. Include optical aerosol spectrometry technology to measure the characteristics of inhaled particles. Evaluate the results and discuss their comparability to findings reported in the available literature.
5. Discuss the obtained results in the context of respiratory research. Outline further directions in modelling of the human respiratory system.

# 1 Breathing simulation using polymer and organic human lung equivalents

## Abstract

Simulation models in respiratory research are increasingly used for medical product development and testing, especially because in vivo models are coupled with a high degree of complexity and ethical concerns. This work introduces a respiratory simulation system, which is bridging the gap between the complex, real anatomical environment and the safe, cost-effective simulation methods. The presented electro-mechanical lung simulator, xPULM™, combines in silico, ex vivo and mechanical respiratory approaches by realistically replicating an actively breathing human lung. The reproducibility of sinusoidal breathing simulations with xPULM™ was verified for selected breathing frequencies (10-18 bpm) and tidal volumes (400-600 mL) physiologically occurring during human breathing at rest. Human lung anatomy was modelled using latex bags and primed porcine lungs. High reproducibility of flow and pressure characteristics was shown by evaluating breathing cycles ( $n_{\text{Total}}=3273$ ) with highest standard deviation  $|3\sigma|$  for both, simplified lung equivalents ( $\mu_{\dot{V}}=23.98\pm 1.04$  L/min,  $\mu_P=-0.78\pm 0.63$  hPa) and primed porcine lungs ( $\mu_{\dot{V}}=18.87\pm 2.49$  L/min,  $\mu_P=-21.13\pm 1.47$  hPa). The adaptability of the breathing simulation parameters, coupled with the use of porcine lungs salvaged from a slaughterhouse process, represents an advancement towards anatomically and physiologically realistic modelling of human respiration.

## Keywords

respiration simulation, biomedical electro-mechanical systems, alternative to animal testing, lung simulation, primed porcine lungs, biomedical engineering education

This chapter is published as:

- R. Pasteka, M. Forjan, S. Sauermann, and A. Drauschke, “Electro-mechanical Lung Simulator Using Polymer and Organic Human Lung Equivalents for Realistic Breathing Simulation,” *Sci. Rep.*, vol. 9, no. 1, p. 19778, Dec. 2019, doi: 10.1038/s41598-019-56176-6.





integrated into the lung simulator, inspired by the functionality of the human respiratory system under physiological conditions. An overview of the simulator setup, depicted in Fig. 1.1, consists of a respiratory-drive system and the rigid thoracic chamber, housing the lung equivalent and mimicing the pressure condition of the thorax. Moreover, the sensors for monitoring pressure, temperature and humidity changes during simulation are included in the thoracic chamber, which is produced out of a transparent Polymethylmethacrylate (PMMA) hosting a total volume of 61 L. This construction allows the simulation process and lung equivalent status monitoring. This feature is particularly useful in training and education.

## 1.2.2 Sinusoidal respiratory simulation

Simulation parameters are chosen to represent physiological value. The simulation parameters were in the following ranges: breathing frequencies (10-18 bpm) and tidal volumes (400-600 mL). Human lung anatomy was modelled using 2x3 L latex bags and primed porcine lungs.

Airflow and pressure characteristics during the simulation in CRC mode were recorded for:

- Sinusoidal breathing pattern with two 3L latex bags in parallel mount.
- Sinusoidal breathing pattern with primed porcine lungs.

## 1.3 Results

### 1.3.1 Evaluation of the breathing simulations

Measurements with xPULM™ are evaluated to assess simulated breathing pattern reproducibility under various conditions. High reproducibility of flow and pressure characteristics was shown by evaluating breathing cycles ( $n_{\text{Total}} = 3273$ ) with the highest standard deviation  $|3\sigma|$  for both, simplified lung equivalents in a form of a latex bag ( $\mu_{\dot{V}} = 23.98 \pm 1.04$  L/min,  $\mu_P = -0.78 \pm 0.63$  hPa) and primed porcine lungs ( $\mu_{\dot{V}} = 18.87 \pm 2.49$  L/min,  $\mu_P = -21.13 \pm 1.47$  hPa).

### 1.3.2 Breathing simulation with the artificial lung equivalent

Analysed airflow characteristics for sinusoidal breathing pattern simulation using latex bags exhibit standard deviation from the mean airflow waveform of  $|3\sigma|$  below 1 L/min for all measured breathing frequencies and tidal volumes. The standard deviation from the mean flow increases slightly with higher breathing frequencies and for greater tidal volumes, reaching the maximum value of 1.04 L/min for  $f = 18$  bpm and  $V_T = 600$  mL. The differences between mean peak inspiratory and expiratory

flows increases with growing breathing frequency. The difference of 7.74 L/min for  $V_T = 600$  mL is highest between breathing frequency of 10 bpm and 18 bpm. A similar trend can be observed in the mean peak expiratory values where the maximal difference is 8.05 L/min for the identical simulation parameters.

Corresponding pressure changes inside the thoracic chamber are characterised by the standard deviation of  $|3\sigma|$  below 0.7 hPa at the local maxima for all measured breathing frequencies and tidal volumes. The mean inspiratory pressure difference of  $-1.20$  hPa and the mean expiratory pressure difference of 0.72 hPa respectively was measured between breathing frequency of 10 bpm and 18 bpm for  $V_T = 600$  mL. Sinusoidal shape of airflow and pressure characteristic is maintained for all measured combinations of tidal volumes and frequencies. Simulation results for volumes varying from 400–600 mL and frequency 12 bpm are depicted in Fig. 1.2. The in-/ex-halation breathing phase lasts the same time duration resulting in an expected inspiration-to-expiration ratio (I:E) of 1:1. Peak inspiratory flow is reached at 25% and the peak expiratory flow at 75% of the breathing cycle. The pressure inside the thoracic chamber oscillates between  $\pm 1.5$  hPa during the sinusoidal breathing cycle simulation. The calculated compliance value for the used latex bags is  $|C_{\text{Latex}}| = \Delta V / \Delta P = 0.51 / 1 \text{ hPa} = 0.5 \text{ L/hPa}$  at peak inspiratory pressure.

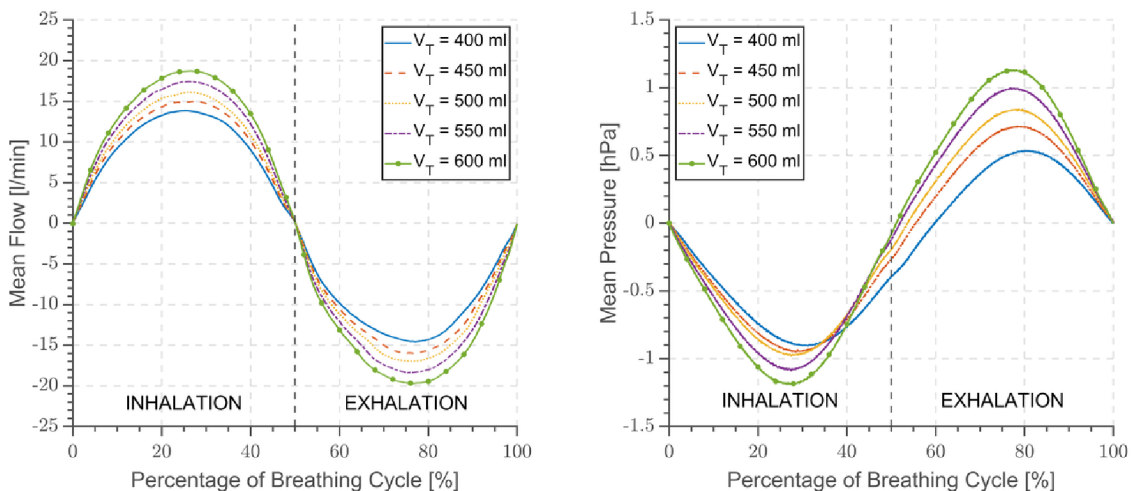


Fig. 1.2: Airflow and pressure characteristics for sinusoidal breathing pattern with frequency 12 bpm, tidal volumes varying from 400–600 mL using two 3 L latex bags in parallel mount as a lung equivalent. The x-axis is normalised in the percentage of breathing cycle where 100% is equivalent to a period of 5 s.

### 1.3.3 Breathing simulation with the primed porcine lungs

The standard deviation of  $|3\sigma|$  below 6 L/min was recorded while using the primed porcine lungs. Increase of a difference between individual cycles can be found under the conditions of low breathing frequencies ( $f = 10$  bpm and 12 bpm) and small tidal volumes ( $V_T = 400$  mL and 450 mL). The difference between mean peak inspiratory and expiratory flow exhibits the same characteristic for both lung equivalents. The maximal difference for peak inspiratory flow is 9.91 L/min and 10.95 L/min for peak expiratory flow between breathing frequency of 10 bpm and 18 bpm for  $V_T = 500$  mL.

Pressure changes recorded with the primed porcine lungs have a standard deviation of  $|3\sigma|$  under 1.5 hPa for all measurement trials. The expiratory peak pressure is below the atmospheric level, preventing the alveolar regions of the lung from collapsing during the breathing cycle. The shift of the mean peak inspiratory pressure towards negative values compensates the elastic properties of the porcine lungs naturally causing them to stay in a collapsed state. Increase of the simulated tidal volume leads to the decrease of the mean peak inspiratory pressure and concurrently causes a rise of the mean peak expiratory pressure. The flow and pressure characteristics are highly reproducible, despite the influence of the tissue properties, and deviate only to a maximum of 2.49 L/min and 1.47 hPa. The calculated compliance value for the included primed porcine lung is  $|C_{\text{Porcine}}| = \Delta V / \Delta P = 0.5 \text{ (L)} / -23.5 \text{ hPa} = 0.02 \text{ L/hPa}$  at peak inspiratory pressure.

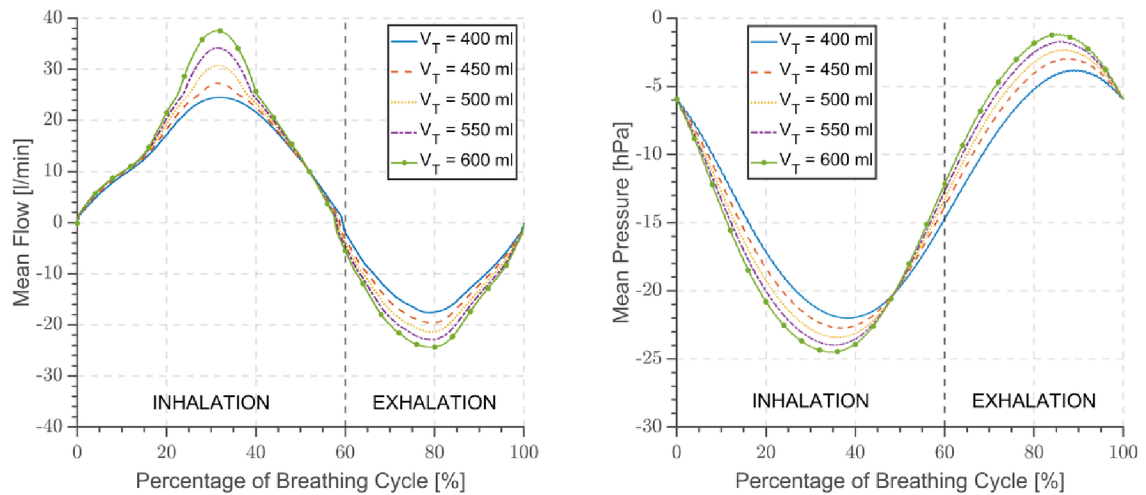


Fig. 1.3: Airflow and pressure characteristics for sinusoidal breathing pattern with frequency 12 bpm, tidal volumes varying from 400–600 mL using primed porcine lungs obtained from a slaughterhouse process. The x-axis is normalised in the percentage of breathing cycle where 100% is equivalent to a period of 5 s.

## 1.4 Discussion

### 1.4.1 Measurements with the latex bags and porcine lungs

The latex bags represent a simplified artificial equivalent of human lungs as they contain no inner structure and have a defined volume. Complex tree-like branching of the primary bronchi, typical for the human lungs, is expressed by the main bifurcation separating the latex bags into a left and a right lung. However, such representation assumes both symmetrical bifurcation and lung lobes. In comparison to the human lung, the resistance of a polymer-based bag as lung equivalent is negligible. The resistance of the simplified simulated respiratory tract, consisting of a y-shaped bifurcation and two symmetrical latex bags, would only influence the performed measurements in case of high flows.

Breathing simulations conducted with the primed porcine lungs are influenced by the properties of the tissue and deviate from the typical sinusoidal curve, as shown in Fig. 1.3. Airflow during the inhalation period increases gradually until the 20% of the breathing cycle is reached. Previously semi-collapsed alveolar regions expand at this point causing a steep increase of flow and prolonged inspiratory breathing phase. This phenomenon is particularly noticeable during simulations with higher tidal volumes. The expiratory breathing phase is shorter as the airflow expelled from the lung is reinforced by the elastic property of the porcine tissue. The I:E ratio varies with increasing tidal volume reaching approximately the value of 2:1 at  $V_T = 600$  mL.

## 1.5 Conclusion

The xPULM™ simulator represents a new approach to the respiratory system behaviour modelling, combining the techniques of *in silico*, *ex vivo* and mechanical models. Measurements of the simulated sinusoidal breathing patterns demonstrate high reproducibility and stability of the system for all five tested tidal volumes at four breathing frequencies. The respiratory simulations were conducted with simplified lung equivalent and primed porcine lungs. Influence of a lung equivalents' mechanical properties on flow and pressure characteristic represents processes naturally occurring during the human respiration cycle.

## 2 Patient-ventilator interaction testing

### Abstract

During mechanical ventilation, a disparity between flow, pressure or volume demands of the patient and the assistance delivered by the mechanical ventilator often occurs. Asynchrony effect and ventilator performance are frequently studied from ICU datasets or using commercially available lung simulators and test lungs. This paper introduces an alternative approach of simulating and evaluating patient-ventilator interactions with high fidelity using the electro-mechanical lung simulator xPULM™ under selected conditions. The xPULM™ approximates respiratory activities of a patient during alternating phases of spontaneous breathing and apnoea intervals while connected to a mechanical ventilator. Focusing on different triggering events, volume assist-controlled (V/A-C) and pressure support ventilation (PSV) modes were chosen to test patient-ventilator interactions. In V/A-C mode a double-triggering was detected every third breathing cycle leading to an asynchrony index of 16.67%, being classified as severe. This asynchrony causes a major increase of Peak Inspiratory Pressure  $PIP = 12.80 \pm 1.39 \text{ cmH}_2\text{O}$  and Peak Expiratory Flow  $PEF = -18.33 \pm 1.13 \text{ L/min}$  when compared to synchronous phases of the breathing simulation. Additionally, events of premature cycling were observed during PSV mode. In this mode, the peak delivered volume during simulated spontaneous breathing phases almost doubles compared to apnoea phases. The presented approach demonstrates the possibility of simulating and evaluating disparities in fundamental ventilation characteristics caused by double-triggering and premature cycling under V/A-C and PSV ventilation modes. Various dynamic clinical situations can be approximated and could help to identify undesired patient-ventilation interactions in the future. Rapidly manufactured ventilator systems could also be tested using this approach.

### Keywords

biomedical engineering, breathing simulation, electro-mechanical lung simulator, patient-ventilator interactions, rapidly manufactured ventilator systems testing

This chapter is published as:

- R. Pasteka, J. P. Santos da Costa, N. Barros, R. Kolar, and M. Forjan, “Patient–Ventilator Interaction Testing Using the Electromechanical Lung Simulator xPULM™ during V/A-C and PSV Ventilation Mode,” *Appl. Sci.*, vol. 11, no. 9, p. 3745, Apr. 2021, doi: 10.3390/app11093745.

## 2.1 Introduction

The functionality of the human respiratory system can be impaired mainly by respiratory pump failure or lung failure. These effects may occur based on a variety of causes like trauma, drug effects, neural damages and other pathologies such as oedema [40]. Respiratory pump failure ultimately leads to the need for controlled or assisted mechanical ventilation, which is meant to support or fully replace spontaneous breathing of a patient providing time for recovery [41]. Assisted mechanical ventilation should be ideally fully adaptive to a patient's respiratory behaviour by providing limited and fully synchronous respiratory support. Otherwise, asynchrony between the patient needs and the output of the ventilator arises [42]. This work aims to introduce a novel approach of simulating and evaluating disparities in fundamental ventilation characteristics using electro-mechanical lung simulator xPULM™ [43].

## 2.2 Materials & Methods

The measurement setup consists of the electro-mechanical lung simulator xPULM™ connected with a standard single-tube to a Bellavista™ 1000 mechanical ventilator (imtmedical, Switzerland). The simulator acts as a ventilated patient and replicates spontaneous sinusoidal breathing while supported by different modes of assisted ventilation. Frequently used volume/assist-control mode (V/A-C) ventilation mode and Pressure Support Ventilation (PSV) modes were chosen in this study as they account for 53% of ventilation modes used in mechanically ventilated and intubated patients [44].

### 2.2.1 Measurement setup & protocol

Two 3 L latex bags with measured compliance  $C_{\text{stat}} = 49 \text{ mL/cmH}_2\text{O}$  and  $C_{\text{dyn}} = 47 \text{ mL/cmH}_2\text{O}$  are used as a lungs equivalent. Additionally, parabolic airway resistance Rp20 (Michigan Instruments, USA) with characteristic similar to that of standard endotracheal tubes is included in the setup.

The xPULM™ simulator acts as a spontaneously breathing human with a breathing frequency of 12 bpm (breaths per minute) and a tidal volume ( $V_T$ ) of 500 mL. The apnoea phase ( $\dot{V} = 0 \text{ L/min}$ ) is introduced after 60 s of sinusoidal spontaneous breathing simulation for a time interval of 60 s. After the apnoea, active spontaneous breathing is resumed, with the same settings, again for a duration of 60 s. The lung simulator and the mechanical ventilator are started consecutively.

The V-A/C mode is operated with the following settings:  $V_T=500$  mL,  $PEEP=0$  cmH<sub>2</sub>O,  $f=12$  bpm,  $T_{\text{insp}}=1.7$  s,  $\text{Flow}_{\text{trigg}}=2.0$  L/min. The PSV mode is operated with the following settings:  $P_{\text{supp}}=10$  cmH<sub>2</sub>O,  $PEEP=0$  cmH<sub>2</sub>O, If apnoea occurs the backup ventilation mode is switched on with  $f=12$  bpm,  $T_{\text{inspMax}}=1.7$  s,  $\text{Flow}_{\text{trigg}}=2.0$  L/min.

### 2.2.2 Asynchrony index

The asynchrony index (AI) for each ventilation mode is calculated across all measurement trials as a number of asynchrony events ( $N_{\text{AE}}$ ) / total respiratory rate ( $\text{RR}_{\text{Total}}$ ) x 100 [45].

## 2.3 Results

The patient-ventilator interaction measurements are separated into two phases and are investigated under two different ventilator modes. The phases are divided into initial spontaneous breathing (SB) performed by the xPULM<sup>TM</sup> simulator (Phase 1), with simulated apnoea (SA) phase in between where the electro-mechanical simulator is not operating (Phase 2).

### 2.3.1 Measurements with V/A-C ventilation mode

The measurements of the xPULM<sup>TM</sup> simulator and the mechanical ventilator operating in V/A-C mode are shown in Fig. 2.1. During Phase 1, the xPULM<sup>TM</sup> is actively breathing while the mechanical ventilator is operating for a period of 60 s. A forced second inhalation cycle is triggered (double triggering) by the mechanical ventilator every third breathing cycle, leading to an abrupt increase of pressure, which is followed by a higher exhalation flow in comparison to the other breathing cycles. With a total amount of 4 asynchronies during the observed time span, the asynchrony index for both phases in V/A-C mode is 16.67%. In the Phase 2, the electro-mechanical simulator was paused to simulate apnoea with the mechanical ventilator taking over the entire breathing effort. Steady breathing cycles can be seen with maximum pressure peaks at the end of the inhalation cycle. To reach the same flow the necessary pressure exerted by the mechanical ventilator doubles in comparison to the Phase 1.

### 2.3.2 Measurements with PSV ventilation mode

In Fig. 2.2, the measurement of interactions between simulated spontaneous breathing and the PSV mode of the mechanical ventilator are depicted. Similarly to the



V/A-C mode the mechanical ventilator is not fully in phase with the lung simulator. The inspiratory time of the lung simulator does not surpass the set maximum inspiratory time threshold of the PSV mode. The delivered peak volume during the active Phases 1 is nearly double than in the apnoea Phase 2. With a total amount of 12 asynchronies during the observed time span, the asynchrony index for both phases in PSV mode is 50%. The effect of asynchronies can be seen in the increased inspiratory flow of both the lung simulator and mechanical ventilator.

### 2.3.3 Comparison of measurements with V/A-C and PSV

The comparison of simulation measurements showing patient-ventilator interactions using different modes of ventilation is summarised in Tab. 2.1. The results exhibit high standard deviations  $\sigma_{\text{FLOW}}$  for inhalation and exhalation peak flow and  $\sigma_{\text{PRESSURE}}$  for inhalation peak pressure in both spontaneous breathing phases during V/A-C mode. The standard deviation for exhalation peak pressure can be neglected for both modes as the PEEP was set to zero. The high standard deviation outcome for V/A-C mode during spontaneous breathing is linked to double triggering which can be seen in Fig. 2.1 for every third breathing cycle. During simulated apnoea in V/A-C mode, the standard deviation  $\sigma_{\text{FLOW}}$  lies below 2.17% for inhalation and exhalation peak flow and  $\sigma_{\text{PRESSURE}}$  lies below 4.42% for inhalation peak pressure. For the PSV mode,  $\sigma_{\text{FLOW}}$  lies below 3.53% for inhalation and exhalation peak flow and  $\sigma_{\text{PRESSURE}}$  lies below 0.41% for inhalation peak pressure when considering both phases.

Tab. 2.1: Patient-ventilator interaction. Differentiation between phases (1: Spontaneous Breathing (SB) and 2: Simulated apnoea (SA)) for both V/A-C and PSV mode with a breathing frequency of 12 bpm.

| Ventilator Mode | Phase | Peak   | Peak  | Peak  | Peak   |
|-----------------|-------|--|---|---|--|
|                 |       | Inspiratory Flow<br>( $\pm\sigma_{\text{FLOW}}$ )<br>[L/min] | Inspiratory Pressure<br>( $\pm\sigma_{\text{PRESSURE}}$ )<br>[cmH <sub>2</sub> O] | Expiratory Flow<br>( $\pm\sigma_{\text{FLOW}}$ )<br>[L/min] | Expiratory Pressure<br>( $\pm\sigma_{\text{PRESSURE}}$ )<br>[cmH <sub>2</sub> O] |
| V/A-C           | SB    | 25.56 ( $\pm 1.34$ )   | 7.96 ( $\pm 6.38$ )   | -25.57 ( $\pm 8.93$ )                                       | 0.14 ( $\pm 0.20$ )  |
|                 | SA    | 26.43 ( $\pm 0.57$ )   | 11.09 ( $\pm 0.49$ )  | -32.9 ( $\pm 0.54$ )  | 0 ( $\pm 0.03$ )   |
| PSV             | SB    | 43.96 ( $\pm 0.01$ )   | 10.18 ( $\pm 0.04$ )  | -27.5 ( $\pm 0.97$ )  | 0.24 ( $\pm 0.08$ )  |
|                 | SA    | 41.19 ( $\pm 0.31$ )   | 10 ( $\pm 0.02$ )   | -32.16 ( $\pm 0.51$ )                                       | 0 ( $\pm 0.03$ )   |

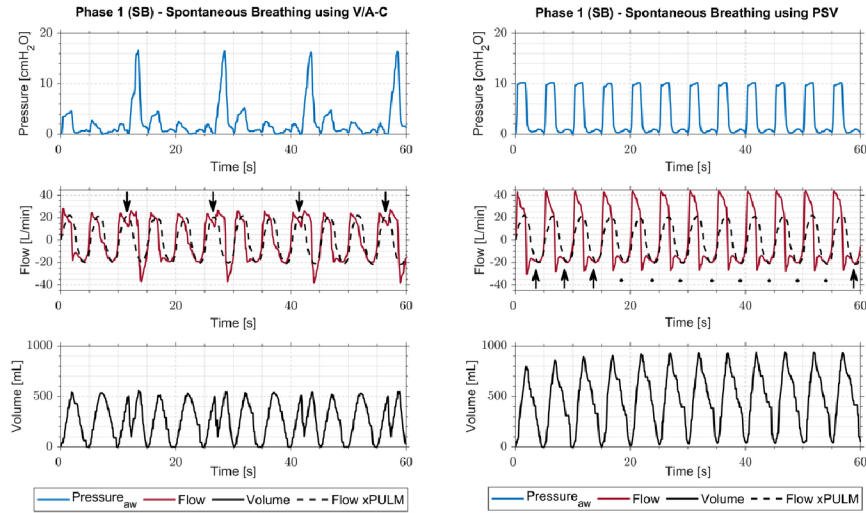


Fig. 2.1: Pressure, flow and volume tracings during spontaneous breathing simulation (SB) phases with the xPULM<sup>TM</sup> and mechanical ventilator BellaVista<sup>TM</sup> in the V/A-C mode (left) and in the PSV mode (right). Simulated patient's breathing frequency is not in phase with the ventilator's frequency representing realistic conditions. This leads to trigger asynchrony (double-triggering) in the V/A-C mode (arrows on the left) and trigger asynchrony (premature cycling) in the PSV mode (arrows on the right).

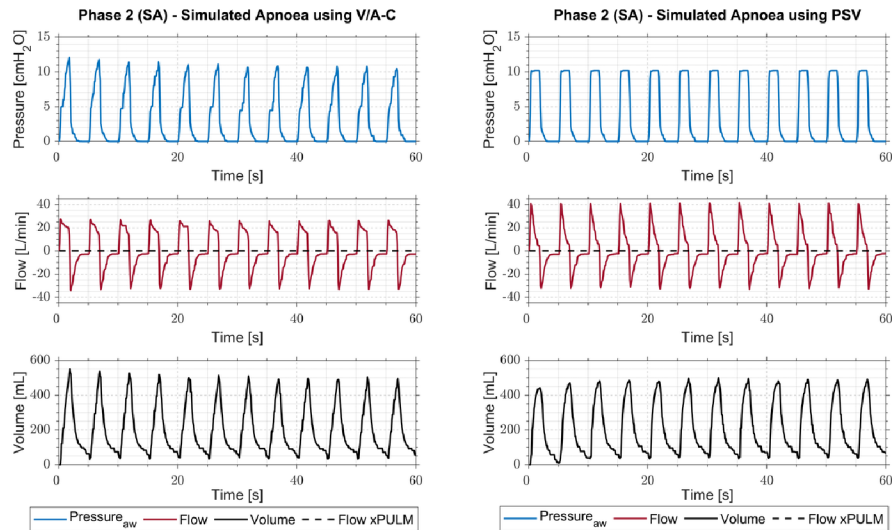


Fig. 2.2: Pressure, flow and volume tracings during simulated apnoea (SA) phase. The xPULM<sup>TM</sup> does not generate any airflow, in this phase, and the mechanical ventilator BellaVista<sup>TM</sup> is overtaking the entire ventilation process using the V/A-C mode (left) and the PSV mode (right).

## 2.4 Discussion

### 2.4.1 Influences of V/A-C and PSV ventilation mode

The first trial show the interaction with the simulated patient during the V/A-C mode. In this case, simulated patient's breathing frequency is not in phase with the ventilator's frequency representing realistic conditions. Patient-ventilator asynchrony can be identified and manifests as a forced second inhalation every third breathing cycle (double-triggering). This event represents a force working against the effort of a spontaneous breathing patient. The mechanical ventilator intervenes despite the patient being sufficiently ventilated. However, this is in concordance with the principle of the V/A-C ventilation mode where the patient always receives at least the set tidal volume. The forced second inhalation, in general, occurs when the ventilator inspiratory time is shorter than the patient's inspiratory time. The results are corresponding with clinical findings reported by Thille et al. [45].

The second trial demonstrate the influence of PSV ventilation mode during simulations of spontaneous breathing and apnoea phases. Mechanical ventilation in PSV mode is supportive but leads to an excessively high peak pressure during spontaneous breathing phases caused by premature cycling. The volume supplied by the mechanical ventilator is compounded to the tidal volume delivered by spontaneous breathing. Consequently, the total volume during SB phases doubles in comparison to the apnoea phases. This leads to insufficient ventilation during the apnoea phases.

## 2.5 Conclusion

In this paper, an approach of testing patient-ventilator interactions using the electro-mechanical lung simulator xPULM™ is introduced. The simulator is used to replicate a spontaneously breathing patient under mechanical ventilation. Overall the presented approach demonstrates the possibility of simulating and evaluating disparities in fundamental ventilation characteristics under V/A-C and PSV ventilation modes.

# 3 Experimental evaluation of dry powder inhalers

## Abstract

Dry powder inhalers are used by a large number of patients worldwide to treat respiratory diseases. The objective of this work is to experimentally investigate changes in aerosol particle diameter and particle number concentration of pharmaceutical aerosols generated by four dry powder inhalers under realistic inhalation and exhalation conditions. To simulate patients undergoing inhalation therapy, the active respiratory system model (xPULM™) was used. A mechanical upper airway model was developed, manufactured and introduced as a part of the xPULM™ to represent the human upper respiratory tract with high fidelity. Integration of optical aerosol spectrometry technique into the setup allowed for evaluation of pharmaceutical aerosols. The results show that there is a significant difference ( $p < 0.05$ ) in mean particle diameter between inhaled and exhaled particles with the majority of the particles depositing in the lung, while particles with the size of ( $>0.5 \mu\text{m}$ ) are least influenced by deposition mechanisms. The fraction of exhaled particles ranges from 2.13% (HandiHaler®) over 2.94% (BreezHaler®), 6.22% (Turbohaler®) to 10.24% (Ellipta®). These values are comparable to previously published studies. Furthermore, the mechanical upper airway model increases the resistance of the overall system and acts as a filter for larger particles ( $>3 \mu\text{m}$ ). In conclusion, the xPULM™ active respiratory system model is a viable option for studying interactions of pharmaceutical aerosols and the respiratory tract regarding applicable deposition mechanisms. The model strives to support the reduction of animal experimentation in aerosol research and provides an alternative to experiments with human subjects.

## Keywords

dry powder inhaler resistance, inspiratory flow rate, inspiratory pressure, aerosol particle deposition, mechanical upper airway model, optical aerosol spectrometry, biomedical engineering

This chapter is published as:

- R. Pasteka, L. Schöllbauer, J. P. Santos da Costa, R. Kolar, and M. Forjan, “Experimental Evaluation of Dry Powder Inhalers During In- and Exhalation Using a Model of the Human Respiratory System (xPULM™),” *Pharm.* 2022, Vol. 14, no. 3, p. 500, Feb. 2022, doi: 10.3390/PHARMACEUTICS14030500.

## 3.1 Introduction

Targeted delivery of pharmaceuticals directly into the affected part of the respiratory region via inhalation drug therapy is crucial for managing cases of obstructive respiratory diseases [18]. The objective of this work is to experimentally investigate changes in aerosol particle diameter and particle number concentration of pharmaceutical aerosols under realistic inhalation and exhalation conditions. In contrast to widely spread measurement setups, this work integrates an optical aerosol spectrometer for inhalation and exhalation measurements to eliminate the drawbacks introduced by cascade impactors [46]. Instead of focusing on PFIR, the focus was put on reaching a pressure drop of at least ( $P_{\text{DROP}} \geq 1$  kPa) for all inhalers.

## 3.2 Materials and Methods

### 3.2.1 Measurement setup and procedure

The following two measurement trials were conducted during this study: A) Characterisation measurements and B) Respiration measurements. To assess the particles generated by the DPIs, Characterisation measurements were performed using a simple connection element to the respiratory model xPULM™. This connector is characterised by a simplified version of the human laryngeal space, in form of a 90 degree bend and includes a sampling nozzle. This aerosol sampling point is in-line with the inhalatory airstream to ensure isoaxial aerosol sampling. Moreover, the control loop of the optical aerosol spectrometer maintains a constant sampling flow, regardless of the inhalation flow profile.

Respiration measurements were conducted to investigate changes in aerosol particle diameter and particle number concentration during inhalation and exhalation. For this purpose, a primed porcine lung was used as a anatomically realistic lung equivalent. The full setup is depicted on Fig. 3.1. The measurement procedure of the Respiration measurements consists of three phases (i) inhalation, (ii) breath-hold, (iii) exhalation. Inhalation with maximum effort was simulated until the pressure drop across the DPI, measured with the FlowAnalyser PF-300 (IMT Analytics, Switzerland), reached at least the recommended pressure drop of  $\geq 1$  kPa [39]. However, if achievable, a pressure drop of 4 kPa, was targeted [47]. The driving force of the inhalation was terminated when the peak value of the pressure drop was reached. However, inhalation continued briefly, due to inertia and compliance of the lung equivalent. Inhaler-specific inhalation profiles were recorded using mass flow sensors SFM3300-AW (Sensirion, Switzerland). The results have been adjusted for the recorded background aerosol load.

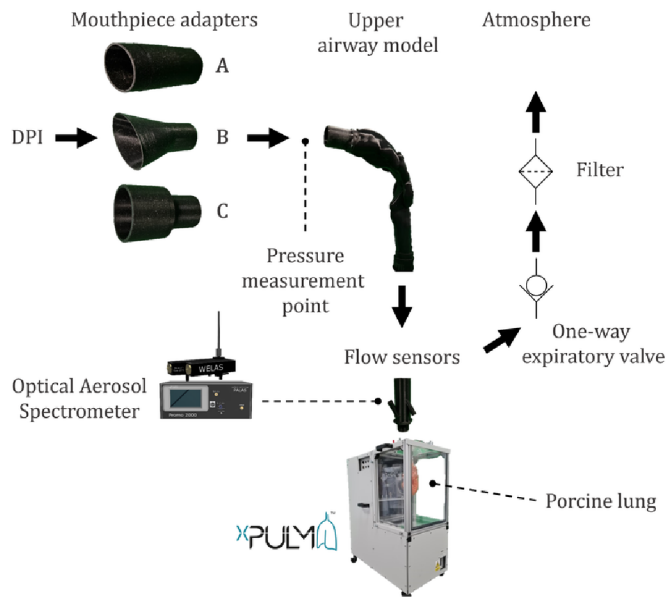


Fig. 3.1: The measurement setup for Respiration measurements consisting of mouth-piece adapters for A) BreezHaler® B) Ellipta®, HandiHaler® C) Turbuhaler®, the mechanical UAM derived from CT examinations, optical aerosol spectrometer used to characterise the aerosol particles and the active model of the human respiratory system xPULM™ with the porcine lung.

The inhalation manoeuvre was followed by a 5 s breath-hold period prior to slow and steady exhalation at a flow of 30 L/min for the duration of 6 s. For each tested DPI, the measurements were repeated 12 times ( $n=12$ ). The in-/exhalation airstream was sampled by the optical aerosol spectrometer Promo 2000 (PALAS, Germany) connected to a white light aerosol sensor Welas 2070 (PALAS, Germany) with a constant flow rate of 5 L/min. The sensor is capable of measuring particles in the range of 0.2  $\mu\text{m}$  to 10  $\mu\text{m}$ .

In total, four DPIs were evaluated in this study, grouped into single-dose and multiple dose inhalers. The single-dose devices (BreezHaler® and HandiHaler®) are loaded with a capsule containing the dose which is punctured prior to use. The remaining three were multi-dose DPIs (Ellipta®, Turbuhaler®) which store multiple doses within the devices. Outlets of all DPIs were modified with custom rapidly manufactured adapters to enable well-fitted, airtight, connection to the oral cavity of the mechanical UAM.

## 3.3 Results and Discussion

### 3.3.1 Inspiratory flow rate and pressure drop measurements

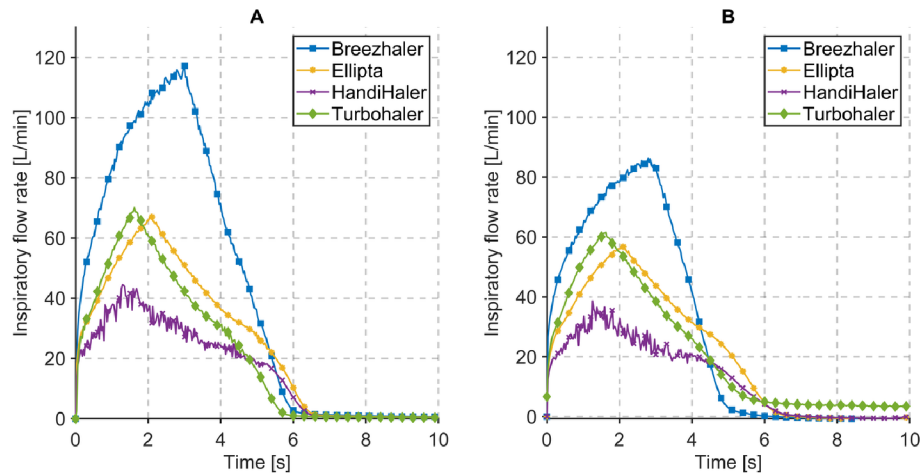


Fig. 3.2: Flow profiles during A) Characterisation measurements B) Respiration measurements while inhaling through Breezhaler®, Ellipta®, HandiHaler® and Turbohaler® at a pressure drop given in Tab. 3.1.

Flow profiles measured during Characterisation and Respiration measurements for the evaluated DPIs are presented in Fig. 3.2. During Characterisation measurements, the resistance of the system is primarily resulting from the inner resistance of the DPIs. The peak inspiratory flow, measured at the pressure drop values, provided in Tab. 3.1, ranges from 45 to 120 L/min. The shape of the inhalation profile, shown in Fig. 3.2A is characteristic for each used DPIs and reflects the individual constructional solution of the devices included in this evaluation.

The inspiratory flow rate during Respiration measurements is influenced by resistance and compliance of the included mechanical UAM and the primed porcine lung, respectively. This is evident for DPIs with low inner resistance (e.g., Breezhaler®) where the inspiratory flow rate drops by 30 L/min. In case of DPIs with higher inner resistance (e.g., HandiHaler®) the flow rate is influenced moderately as the increase of the overall system resistance is lower. The peak inspiratory flow, measured at the pressure drop values, provided in Tab. 3.1, ranges from 39 to 86 L/min. The system resistance refers to a combination of DPI inner resistance (constant) and the resistance of attached pneumatic components.

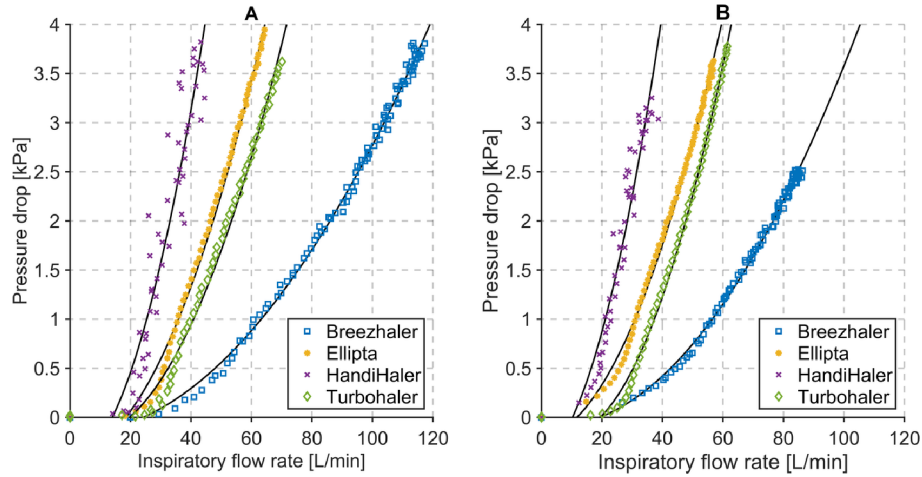


Fig. 3.3: Relationships between inspiratory flow and pressure drop of four commercial DPIs during A) Characterisation measurements B) Respiration measurements.

### 3.3.2 Influence of the UAM and the primed porcine lung

Effects of the mechanical UAM and the primed porcine lung during Respiration measurements are evident from the relationship between inspiratory flow rate and pressure drop across the inhalers, see Fig. 3.3B. The resistance of the measurement system increases significantly ( $p < 0.05$ ) with all inhalers (see Tab. 3.1) and a pressure drop of 4 kPa is reached for lower inspiratory flow rates.

The measurements revealed limitations in reaching the pressure drop of 4 kPa consistently for Breezhaler®. The position of the capsule within the DPI, as well as the angle of the device are critical.

Relevant parameter values for the used DPIs, Characterisation measurements and Respiration measurements are summarised in Tab. 3.1. These parameter values complement the graphical result shown in Fig. 3.2 and Fig. 3.3.

Tab. 3.1: Summary of the relevant parameter values for the used DPIs where:  $V_{INH}$  - inhaled volume,  $P_{DROP}$  - pressured drop across the inhaler during inhalation, PIF - peak inspiratory flow, and  $t_{INH}$  - inhalation time.

| Dry powder inhalers    | Characterisation parameters |                  |                     |                |                  | Respiration parameters                           |                  |                     |                |                  |
|------------------------|-----------------------------|------------------|---------------------|----------------|------------------|--|------------------|---------------------|----------------|------------------|
|                        | Device                      | $V_{inh}$<br>[L] | $P_{DROP}$<br>[kPa] | PIF<br>[L/min] | $t_{inh}$<br>[s] | System Resistance<br>[kPa <sup>1/2</sup> /L/min] | $V_{inh}$<br>[L] | $P_{DROP}$<br>[kPa] | PIF<br>[L/min] | $t_{inh}$<br>[s] |
| Seebri® Breezhaler®    | 6.98                        | 3.81             | 117.28              | 3.00           | 0.0166           | 4.55   | 2.52             | 86.31               | 3.00           | 0.0184*          |
| Anoro® Ellipta®        | 4.06                        | 4.27             | 67.01               | 2.10           | 0.0308           | 3.38   | 3.63             | 56.94               | 2.10           | 0.0335*          |
| Spiriva® HandiHaler®   | 2.60                        | 3.82             | 44.50               | 1.40           | 0.0439           | 2.05   | 3.25             | 38.62               | 1.40           | 0.0467*          |
| Symbicort® Turbohaler® | 3.52                        | 3.83             | 70.11               | 1.60           | 0.0279           | 3.40   | 3.89             | 61.48               | 1.60           | 0.0320*          |

\*  $p < 0.05$  for difference between resistances measured with and without the mechanical UAM



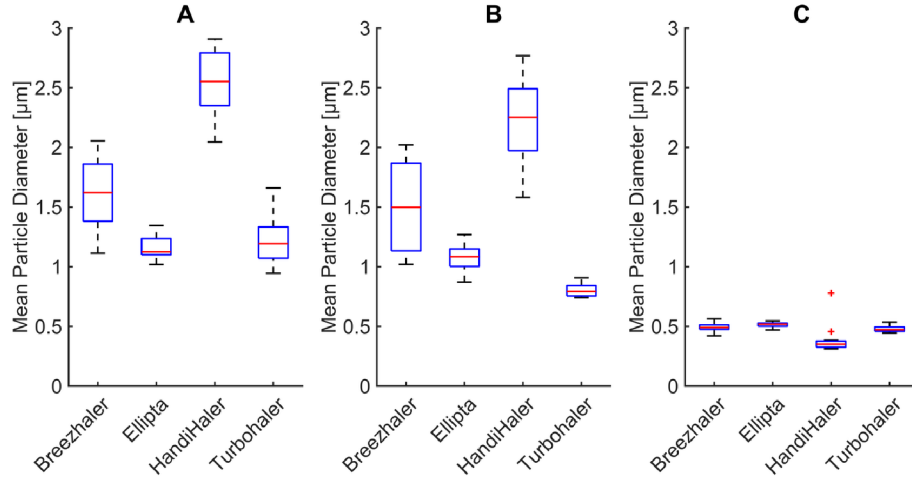


Fig. 3.4: Changes in mean particle diameter during A) Characterisation B) Inhalation C) Exhalation measurements for four commercial DPIs

### 3.3.3 Changes in mean particle diameter

Changes in mean particle diameter ( $M_1$ ) during DPI Characterisation and Respiration measurements using the mechanical UAM and primed porcine lung are depicted in Fig. 3.4. During characterisation measurements the mean particle diameter ranges from  $0.95 \mu\text{m}$  (TurboHaler®) to  $2.90 \mu\text{m}$  (HandiHaler®). These results are comparable to literature values reporting particles ranging from  $2.20 \mu\text{m}$  (Ellipta®) to  $3.90 \mu\text{m}$  (HandiHaler®) [48]. Filtration properties of the mechanical UAM cause the mean particle diameter to shift towards lower values during inhalation.

Exhaled particles during our measurements are characterised by a mean particle diameter in a narrow range from  $0.31 \mu\text{m}$  (HandiHaler®) to  $0.56 \mu\text{m}$  (BreezHaler®). These results were expected as the deposition of aerosol particles in the lung reaches its minimum at  $0.5 \mu\text{m}$  [49]. Furthermore, there is a significant difference ( $p < 0.05$ ) in mean particle diameter between inhaled and exhaled particles Fig. 3.4B & C for all tested DPIs (K-W test,  $H = 17.29$ ,  $p = 0.00003$ ). This change is caused by the interaction of the aerosol particles with the primed porcine lung tissue.

### 3.3.4 Deposition of particles in the porcine lung

The difference between the particle number concentration in inhaled and exhaled air can be considered as number concentration of particles depositing in the porcine lung. The measured particle size distribution for Ellipta and Turbohaler during inhalation is characterised by lower mean particle diameters ( $1.08 \mu\text{m}$  and  $0.79 \mu\text{m}$  respectively). The deposition can be expressed as a percentage of particle number concentration averaged over the individual inhalation or exhalation cycles. All mea-

sured DPIs show deposition above 80% achieving the intended drug delivery. There is a statistically significant difference ( $p < 0.05$ ) between particle number concentration in inhaled and exhaled airstream for all tested inhalers (K-W test,  $H = 17.29$ ,  $p = 0.00003$ ). This is caused by particles depositing in the primed porcine lung.

The generated drug particles from the DPIs are inhaled through the mechanical UAM which represents the naso-oro-pharyngo-laryngeal region (extrathoracic region). Larger particles ( $>3\mu\text{m}$ ) deposit in this region mainly due to effects of inertial impaction [49]. The rest of the drug particles penetrates the deeper regions of the respiratory tract model and reach the primed porcine lung.

Regional lung deposition and bronchodilator response of pharmaceutical aerosols was studied extensively in previous works [50], [51]. Their results confirm that small particles are exhaled with exhalation fractions for particle diameters  $1.5\mu\text{m}$ ,  $3\mu\text{m}$  and  $6\mu\text{m}$  being 22%, 8%, and 2% respectively [51]. A lung deposition study in healthy human subjects showed a exhalation fraction of exhaled dose of 1.2% [50].

The fraction of exhaled particles reported in [52] ranges between 1.6% and 3.3%. These findings are consistent with our measurements where the fraction of exhaled particles ranges from 2.13% (HandiHaler®), 2.94% (BreezHaler®), 6.22% (Turbohaler®) to 10.24% (Ellipta®).

### 3.4 Summary and Conclusion

In this work, aerosol particle diameter and particle number concentration of pharmaceutical aerosols generated by four commercially available DPIs were investigated.

Our results can be summarised as follows:

- Integration of a mechanical UAM, as a part of the xPULM™, increases the resistance of the overall system.
- Inclusion of a porcine lung as a representation of the human lower respiratory tract (compliant with the 3R principles) allows comparable particle deposition to reported findings [50]–[52].
- Mean particle diameter is reduced by the filtration properties of the mechanical UAM, affecting mostly larger particles ( $>3\mu\text{m}$ ). Such models, when based on CT examinations, are reliably representing the function of the human upper respiratory tract.
- The majority of particles entering the porcine lung deposit within, minimum deposition is reached for the particle size of ( $0.5\mu\text{m}$ ). The primed porcine lung is therefore a suitable lung equivalent and representation of the human lung.
- Sampling of the airstream during inhalation and exhalation and its subsequent evaluation using optical aerosol spectrometry techniques is a viable alternative to impactors for evaluating pharmaceutical aerosols.

## Further directions & future work

Due to the rapid advancements in the underlying technology (e.g. CFD and microfluidics), *in silico* and *in vitro* organ-on-a-chip models of the human respiratory system are the most prominent in the research landscape. These models facilitate developments in applications such as drug development and toxicity testing. Nevertheless, *in silico* models are limited by challenges of simulating turbulent and transitional flows, static boundary conditions (airway expands during inhalation) and require simplifications of respiratory system geometry. Furthermore, there is a need to validate such models experimentally. *In vitro* models lack a systemic response, have difficulties to capturing interactions between different cell types and the impact of long term exposure and must cope with a limited lifespan of the used cells. Other, complementary modelling approaches fill the gaps resulting from these limitations. Every modelling approach has advantages and disadvantages. It is the combination of findings from each of them that allows for continuous advancements in respiratory research.

Further directions include:

- Implementation of new technologies to the existing models and creation of new models to allow for high-fidelity simulation representing in realistic manner anatomy, physiology, and pathophysiology of the human respiratory system.
- Personalised approaches in medicine where patient-specific respiratory patterns, airway geometry and lung condition are being simulated to achieve the best possible result for the individual.
- Research of novel methods in guided pulmonary drug delivery, drug formulation, and inhalation of antibiotics, biopharmaceuticals or anti-cancer treatment.
- Compliance and the advancements of the 3R principles (Replace, Reduce, Refine) of humane animal research being at the forefront of all modern research endeavours.

This thesis can be seen as one of the major steps on the path to further research of clinically relevant applications of the xPULM™. The results of the thesis enable advances in research focusing on breathing simulations with other animal lungs (e.g. rabbit, sheep), development of different UAM with various manufacturing mechanisms and materials, testing of additional medical aerosol generators such as nebulisers, and implementation of new aerosol measurement techniques. Building on the presented work, new research projects are currently underway and focus on the development of novel treatment options in neonatal care, methods to minimise patient-ventilator asynchronies, comparison of different upper airway geometries, and determination of local aerosol particle deposition in the lungs.

# Conclusion

This thesis aims to establish a physical model of the human respiratory system (xPULM™) that represents an innovative approach to respiratory system behaviour modelling. To reach this aim, three clinically relevant applications were researched, namely (i) breathing simulation, (ii) patient-ventilator interaction testing and (iii) aerosolised drug delivery. These applications reflect state-of-the-art directions in which respiratory system models are being used.

First, the reproducibility of sinusoidal breathing simulation has been verified for a range of physiological tidal volumes and frequencies. The xPULM™ simulator represents an innovative approach to the respiratory system behaviour modelling and is capable of simulating different breathing patterns with high fidelity. The possibility of using lung equivalents such as polymer-based breathing bags or animal lungs is unique and allows for the representation of processes naturally occurring during the human respiration cycle. The breathing simulation reliably captures flow and pressure changes representative of those occurring during human breathing.

Second, a new approach of testing patient-ventilator interactions using the xPULM™ simulator has been introduced. The results show that different asynchronies can be triggered when the simulator is used to represent a patient undergoing assisted mechanical ventilation. This approach can support identification, investigation and testing of undesired patient-ventilation interactions and contribute to efforts minimising their occurrences, increasing the well-being of patients.

Third, the number concentration and size distribution of aerosol particles generated by commonly used dry powder inhalers have been experimentally evaluated. Investigation of the characteristics of the particles under realistic inhalation and exhalation is possible due to the inclusion of an optical aerosol spectrometer. This technique is not routinely used for such purposes and provides insights into the interactions of aerosol particles in the porcine lungs during breathing. Additionally, a mechanical upper airway model was developed, manufactured, and introduced as a part of the xPULM™. The model was derived from CT examinations and is representative of realistic airway geometry. This approach proposes an alternative to animal experimentation suitable for applications in aerosol research.

The results of this thesis are embedded in teaching and research activities at the University of Applied Sciences Technikum Wien. Additionally, this thesis contributes to the continuous collaboration between the University of Applied Sciences Technikum Wien, Brno University of Technology and other institutions.

In conclusion, the set objectives of the dissertation have been met. The thesis contains original research that has been presented at international conferences and published in three impact factor journals.

## Bibliography

- [1] K. Harper and G. Armelagos, “The changing disease-scape in the third epidemiological transition”, *International Journal of Environmental Research and Public Health* 2010, Vol. 7, Pages 675-697, vol. 7, pp. 675–697, 2 Feb. 2010, ISSN: 16604601. DOI: 10.3390/IJERPH7020675.
- [2] M. Wahdan, “The epidemiological transition”, *Eastern Mediterranean Health Journal*, pp. 8–20, 1996, ISSN: 1687-1634. DOI: <https://doi.org/10.26719/1996.2.1.8>.
- [3] W. H. Organisation, *World health statistics 2021: monitoring health for the SDGs, sustainable development goals*, 12. World Health Organisation, 2021, vol. 58, ISBN: 9789240027053.
- [4] A. P. Roth, C. F. Lange, and W. H. Finlay, “The effect of breathing pattern on nebulizer drug delivery.”, *Journal of aerosol medicine : the official journal of the International Society for Aerosols in Medicine*, vol. 16, no. 3, pp. 325–339, 2003. DOI: 10.1089/089426803769017677.
- [5] W. H. Organization, “Towards the end of the epidemics: First progress report”, en, World Health Organization, Geneva, Tech. Rep., 2017.
- [6] OECD, *Health at a Glance 2019: OECD Indicators*, ser. Health at a Glance. OECD, Nov. 7, 2019, ISBN: 9789264382084. DOI: 10.1787/4dd50c09-en.
- [7] G. A. Network, *The Global Asthma Report 2018*. Auckland, New Zealand, ISBN: 9780473465230.
- [8] F. of International Respiratory Societies, *The Global Impact of Respiratory Disease*. European Respiratory Society, 2017.
- [9] W. H. Organization, *Assessing national capacity for the prevention and control of noncommunicable diseases: report of the 2019 global survey*. Geneva: World Health Organization, 2020, Section: ix, 101 p., ISBN: 9789240002319.
- [10] OECD, *Health at a Glance 2021*, ser. Health at a Glance. OECD, Nov. 2021, ISBN: 9789264961012. DOI: 10.1787/ae3016b9-en.
- [11] P. M. Lepper and R. M. Muellenbach, “Mechanical ventilation in early covid-19 ards”, *EClinicalMedicine*, vol. 28, p. 100616, Nov. 2020, ISSN: 2589-5370. DOI: 10.1016/J.ECLINM.2020.100616.
- [12] C. Roussos and A. Koutsoukou, “Respiratory failure”, *Eur Respir J*, vol. 22, pp. 3–14, 2003. DOI: 10.1183/09031936.03.00038503.

- [13] C. de Haro, L. Sarlabous, J. Esperanza, *et al.*, in *ERS practical Handbook of Invasive Mechanical Ventilation*, M. J. S. Leo Heunks, Ed. The European Respiratory Society, 2019, ch. Monitoring patient-ventilator interaction. DOI: 10.1183/9781849841221.eph01.
- [14] C. de Haro, A. Ochagavia, J. López-Aguilar, *et al.*, “Patient-ventilator asynchronies during mechanical ventilation: Current knowledge and research priorities”, *Intensive Care Medicine Experimental*, vol. 7, no. S1, 2019, ISSN: 2197-425X. DOI: 10.1186/s40635-019-0234-5.
- [15] J. Bousquet and N. Kaltaev, “Global surveillance, prevention and control of chronic respiratory diseases : A comprehensive approach / edited by Jean Bousquet and Nikolai Khaltaev”, en, *A word where all people breathe freely*, 2007, Place: Geneva Publisher: World Health Organization Section: vii, 146 p., ISSN: 9789241563468.
- [16] M. B. Dolovich and R. Dhand, “Aerosol drug delivery: Developments in device design and clinical use”, *The Lancet*, vol. 377, pp. 1032–1045, 9770 Mar. 2011, ISSN: 0140-6736. DOI: 10.1016/S0140-6736(10)60926-9.
- [17] S. W. Stein and C. G. Thiel, “The History of Therapeutic Aerosols: A Chronological Review”, en, *Journal of Aerosol Medicine and Pulmonary Drug Delivery*, vol. 30, no. 1, pp. 20–41, Feb. 2017, ISSN: 1941-2711, 1941-2703. DOI: 10.1089/jamp.2016.1297.
- [18] C. Sorino, S. Negri, A. Spanevello, *et al.*, “Inhalation therapy devices for the treatment of obstructive lung diseases: The history of inhalers towards the ideal inhaler”, *European Journal of Internal Medicine*, vol. 75, pp. 15–18, May 2020, ISSN: 0953-6205. DOI: 10.1016/J.EJIM.2020.02.023.
- [19] M. Sakagami, “In vivo, in vitro and ex vivo models to assess pulmonary absorption and disposition of inhaled therapeutics for systemic delivery”, *Advanced drug delivery reviews*, vol. 58, pp. 1030–1060, 9-10 Oct. 2006, ISSN: 0169-409X. DOI: 10.1016/J.ADDR.2006.07.012.
- [20] J. D. Harding, “Nonhuman Primates and Translational Research: Progress, Opportunities, and Challenges”, *ILAR Journal*, vol. 58, no. 2, pp. 141–150, 2017, ISSN: 1084-2020. DOI: 10.1093/ilar/ilx033.
- [21] S. Festing and R. Wilkinson, “The ethics of animal research. talking point on the use of animals in scientific research”, *EMBO reports*, vol. 8, no. 6, pp. 526–530, Jun. 2007, 17545991[pmid], ISSN: 1469-221X. DOI: 10.1038/sj.embor.7400993.

- [22] W. M. S. Russell and R. L. Burch, *The principles of humane experimental technique*, English. Methuen London, 1959, 238 p. DOI: <https://doi.org/10.5694/j.1326-5377.1960.tb73127.x>.
- [23] V. Monamy, *Animal Experimentation*. Cambridge University Press, 2017, ISBN: 9781316678329. DOI: 10.1017/9781316678329.
- [24] E. Council and E. Parliament, “Caring for animals aiming for better science”, *Official Journal of the European Union*, pp. 1–162, 2010.
- [25] F. Gruber and T. Hartung, “Alternatives to animal experimentation in basic research”, *Altex*, vol. 21, no. Suppl 1/04, pp. 3–31, Oct. 2004.
- [26] N. T. Nguyen, S. A. M. Shaegh, N. Kashaninejad, and D. T. Phan, “Design, fabrication and characterization of drug delivery systems based on lab-on-a-chip technology”, *Advanced Drug Delivery Reviews*, vol. 65, no. 11-12, pp. 1403–1419, 2013, ISSN: 0169409X. DOI: 10.1016/j.addr.2013.05.008.
- [27] D. Wang, Y. Cong, Q. Deng, *et al.*, “Physiological and disease models of respiratory system based on organ-on-a-chip technology”, *Micromachines 2021, Vol. 12, Page 1106*, vol. 12, p. 1106, 9 Sep. 2021, ISSN: 2072666X. DOI: 10.3390/MI12091106.
- [28] J. W. Yang, Y. C. Shen, K. C. Lin, *et al.*, “Organ-on-a-chip: Opportunities for assessing the toxicity of particulate matter”, *Frontiers in Bioengineering and Biotechnology*, vol. 8, p. 519, May 2020, ISSN: 22964185. DOI: 10.3389/FBIOE.2020.00519/BIBTEX.
- [29] N. Khalid, I. Kobayashi, and M. Nakajima, “Recent lab-on-chip developments for novel drug discovery”, *Wiley Interdisciplinary Reviews: Systems Biology and Medicine*, vol. 9, e1381, 4 Jul. 2017, ISSN: 1939-005X. DOI: 10.1002/WSBM.1381.
- [30] B. Palsson, “The challenges of in silico biology”, *Nature Biotechnology*, vol. 18, pp. 1147–1150, 11 Nov. 2000, ISSN: 1087-0156. DOI: 10.1038/81125.
- [31] ICRP, “Human respiratory tract model for radiological protection”, *Radiation Protection Dosimetry*, vol. 60, no. 4, pp. 307–310, Jul. 1995, ISSN: 1742-3406. DOI: 10.1093/oxfordjournals.rpd.a082732.
- [32] N. C. on Radiation Protection and M. (U.S.), *Mammography: recommendations of the National Council on Radiation Protection and Measurements*, 66. The Council, 1980, p. 85, ISBN: 0913392510.

- [33] V. K. H. Bui, J. Y. Moon, M. Chae, *et al.*, “Prediction of aerosol deposition in the human respiratory tract via computational models: A review with recent updates”, *Atmosphere*, vol. 11, no. 2, 2020, ISSN: 20734433. DOI: 10.3390/atmos11020137.
- [34] R. U. Agu and M. I. Ugwoke, “In situ and ex vivo nasal models for preclinical drug development studies”, *Drug Absorption Studies*, pp. 112–134, Dec. 2008. DOI: 10.1007/978-0-387-74901-3\_5.
- [35] “Efficacy of milk-derived bioactive peptides on health by cellular and animal models”, *Nutrients in Dairy and Their Implications for Health and Disease*, pp. 303–311, Jan. 2017. DOI: 10.1016/B978-0-12-809762-5.00023-1.
- [36] R. Nossa, J. Costa, L. Cacopardo, and A. Ahluwalia, “Breathing in vitro: Designs and applications of engineered lung models.”, *Journal of tissue engineering*, vol. 12, p. 20417314211008696, Apr. 2021, ISSN: 2041-7314. DOI: 10.1177/20417314211008696.
- [37] S. Heili-Frades, G. Peces-Barba, and M. J. Rodriguez-Nieto, “Design of a lung simulator for teaching lung mechanics in mechanical ventilation”, *Arch Bronconeumol.*, vol. 43, no. 12, pp. 674–679, Dec. 2007. DOI: 10.1157/13112966.
- [38] E. L’Her, A. Roy, and N. Marjanovic, “Bench-test comparison of 26 emergency and transport ventilators”, *Critical Care*, vol. 18, no. 5, pp. 1–14, 2014, ISSN: 1466609X. DOI: 10.1186/s13054-014-0506-0.
- [39] A. R. Clark, J. G. Weers, and R. Dhand, “The confusing world of dry powder inhalers: It is all about inspiratory pressures, not inspiratory flow rates”, *Journal of Aerosol Medicine and Pulmonary Drug Delivery*, vol. 33, no. 1, pp. 1–11, 2020, ISSN: 19412703. DOI: 10.1089/jamp.2019.1556.
- [40] R. Scala and L. Heunks, “Highlights in acute respiratory failure”, *European Respiratory Review*, vol. 27, no. 147, Mar. 2018, ISSN: 16000617. DOI: 10.1183/16000617.0008-2018.
- [41] T. Pham, L. J. Brochard, and A. S. Slutsky, *Mechanical ventilation: State of the art*, Sep. 2017. DOI: 10.1016/j.mayocp.2017.05.004.
- [42] R. M. Kacmarek, M. Pirrone, and L. Berra, *Assisted mechanical ventilation: The future is now!*, Jul. 2015. DOI: 10.1186/s12871-015-0092-y.
- [43] R. Pasteka, M. Forjan, S. Sauermann, and A. Drauschke, “Electro-mechanical lung simulator using polymer and organic human lung equivalents for realistic breathing simulation”, *Scientific Reports*, vol. 9, no. 1, pp. 1–12, 2019. DOI: 10.1038/s41598-019-56176-6.



- [44] P. G. Metnitz, B. Metnitz, R. P. Moreno, *et al.*, “Epidemiology of mechanical ventilation: Analysis of the saps 3 database”, *Intensive Care Medicine*, vol. 35, no. 5, pp. 816–825, Mar. 2009, ISSN: 14321238. DOI: 10.1007/s00134-009-1449-9.
- [45] A. W. Thille, P. Rodriguez, B. Cabello, *et al.*, “Patient-ventilator asynchrony during assisted mechanical ventilation”, *Intensive Care Medicine*, vol. 32, no. 10, pp. 1515–1522, Oct. 2006, ISSN: 03424642. DOI: 10.1007/s00134-006-0301-8.
- [46] M. Bonam, D. Christopher, D. Cipolla, *et al.*, “Minimizing variability of cascade impaction measurements in inhalers and nebulizers”, *AAPS PharmSciTech*, vol. 9, pp. 404–413, 2 Jun. 2008, ISSN: 15309932. DOI: 10.1208/S12249-008-9045-9.
- [47] U. S. P. Convention, *USP35 NF30, 2012: <601> Aerosols, Nasal Sprays, Metered-Dose Inhalers, and Dry Powder Inhalers*, ser. The United States pharmacopeia. United States Pharmacopeial, 2011, ISBN: 9781936424009.
- [48] A. Horváth, I. Balásházy, G. Tomisa, and Á. Farkas, “Significance of breath-hold time in dry powder aerosol drug therapy of copd patients”, *European Journal of Pharmaceutical Sciences*, vol. 104, no. April, pp. 145–149, 2017, ISSN: 18790720. DOI: 10.1016/j.ejps.2017.03.047.
- [49] C. Darquenne, “Aerosol deposition in health and disease”, *Journal of Aerosol Medicine and Pulmonary Drug Delivery*, vol. 25, no. 3, pp. 140–147, 2012, ISSN: 19412711. DOI: 10.1089/jamp.2011.0916.
- [50] S. Newman, S. Malik, P. Hirst, *et al.*, “Lung deposition of salbutamol in healthy human subjects from the maghaler dry powder inhaler”, *Respiratory Medicine*, vol. 96, no. 12, pp. 1026–1032, 2002, ISSN: 09546111. DOI: 10.1053/rmed.2002.1387.
- [51] O. S. Usmani, M. F. Biddiscombe, and P. J. Barnes, “Regional lung deposition and bronchodilator response as a function of  $\beta$ 2-agonist particle size”, *American Journal of Respiratory and Critical Care Medicine*, vol. 172, no. 12, pp. 1497–1504, 2005, ISSN: 1073449X. DOI: 10.1164/rccm.200410-14140C.
- [52] J. C. Virchow, G. Poli, C. Herpich, *et al.*, “Lung Deposition of the Dry Powder Fixed Combination Beclometasone Dipropionate Plus Formoterol Fumarate Using NEXThaler® Device in Healthy Subjects, Asthmatic Patients, and COPD Patients”, *Journal of Aerosol Medicine and Pulmonary Drug Delivery*, vol. 31, no. 5, pp. 269–280, 2018, ISSN: 19412703. DOI: 10.1089/jamp.2016.1359.

## Curriculum Vitae

**Richard Paštěka**

+43 67761784057

RichardPasteka@gmail.com

Date of birth: 3 May 1991

Nationality: Czech

### RELEVANT EXPERIENCE

---

Since 08/2016  
Vienna, Austria

**University of Applied Sciences Technikum Wien**

*Researcher & Lecturer*

- Is an institutional project lead in the Horizont2020 project “European mHealthHub” (leading institutions are WHO and ITU)
- Is an institutional project lead in the Erasmus+ project “MedTec+”
- Is responsible for teaching and research in the Medical Devices & Cardiopulmonary Simulation Laboratory. Focus: modelling and simulation of the human respiratory system and aerosol science
- Contributes to the coordination of activities in the master study program “Medical Engineering & eHealth”, and internationalization effort at the UAS Technikum Wien
- Contributed to research projects: IES, REHABitation, HealthConnect

### EDUCATION

---

Since 09/2016  
Brno, Czech Republic

**Brno University of Technology**

*Doctoral Degree in Biomedical Technologies*

- Focuses on modelling and simulation of the human respiratory system and aerosol science

01/2014 – 06/2016

**Brno University of Technology, University of Applied Sciences Technikum Wien**

Vienna, Austria

*Ing. and MSc. in Biomedical and Ecological Engineering*

- Master’s Thesis: Integration and Testing of a Real-Time Processing Unit for Lung Simulation. Graduated with the highest distinctions
- The first student of the Double Degree program established between the Brno University of Technology and the University of Applied Sciences Technikum Wien
- Received 1st-grade scholarship for outstanding study results in all semesters

09/2011 – 05/2014  
Brno, Czech Republic

**Brno University of Technology**

*BSc. in Biomedical Technology and Bioinformatics*

- Bachelor’s Thesis: Oscilloscope with the Android Operating System
- Received scholarship for outstanding study results (5th and 6th semester)

## SELECTED PUBLICATIONS

---

R. Pasteka, M. Forjan, S. Sauermann, and A. Drauschke, “Electromechanical Lung Simulator Using Polymer and Organic Human Lung Equivalents for Realistic Breathing Simulation,” *Sci. Rep.*, vol. 9, no. 1, Dec. 2019, doi: 10.1038/s41598-019-56176-6.

R. Pasteka, J. P. Santos da Costa, N. Barros, R. Kolar, and M. Forjan, “Patient–Ventilator Interaction Testing Using the Electromechanical Lung Simulator xPULMTM during V/A-C and PSV Ventilation Mode,” *Appl. Sci.*, vol. 11, no. 9, p. 3745, Apr. 2021, doi: 10.3390/app11093745.

R. Pasteka, L. Schöllbauer, J. P. Santos da Costa, R. Kolar, and M. Forjan, “Experimental Evaluation of Dry Powder Inhalers During In- and Exhalation Using a Model of the Human Respiratory System (xPULMTM),” *Pharm.* 2022, Vol. 14, Page 500, vol. 14, no. 3, p. 500, Feb. 2022, doi: 10.3390/PHARMACEUTICS14030500.

## SKILLS

---

|                     |   |
|---------------------|---|
| <b>Certificates</b> | Quality & Regulatory Affairs Manager-Junior for Medical Products Certificate (TÜV Austria)<br>International Teaching Certificate (FHTW)<br>Cross-Cultural Competences and Language Certificate (FHTW) |
| <b>Languages</b>    | Czech (mother tongue), English (C1), German (B1)  |

## TRAINING & ACTIVITIES

---

|  |  |
|--|--|
| 05/2021<br>Vila Real, Portugal           | <b>Vienna University of Technology</b><br><i>Invited Lecture</i> <ul style="list-style-type: none"><li>Lecture titled “Applications of human respiratory system modelling in the context of biomedical engineering“</li></ul>                                |
| 06/2019<br>Vila Real, Portugal           | <b>University of Vienna</b><br><i>Participant at Basic Aerosol Science Summer School</i> <ul style="list-style-type: none"><li>Reinforcement of principles and techniques utilised in aerosol science.</li></ul>   |
| 11/2018 – 12/2018<br>Vila Real, Portugal | <b>Centro Hospitalar De Trás-Os-Montes E Alto Douro</b><br><i>Visiting Researcher</i> <ul style="list-style-type: none"><li>Data acquisition and analysis of respiratory data at the Department of Pulmonology</li></ul>                                     |
| 12/2018 & 08/2019<br>Vila Real, Portugal | <b>University of Trás-os-Montes and Alto Douro</b><br><i>Invited Lectures</i> <ul style="list-style-type: none"><li>2018 Lecture titled “Human Respiratory System Modelling”</li><li>2019 Lecture titled “Applications of BME in Respiratory Care”</li></ul> |

# Abstract

The increasing incidence of respiratory diseases burdens the world's population and drives major scientific advances in the area of respiratory research. Various models of the human respiratory system are being developed to increase the knowledge and to allow for studies of specific research questions. This thesis aims to establish a physical model of the human respiratory system (xPULM™) that represents an innovative approach to respiratory system behaviour modelling.

To reach this aim, three clinically relevant applications were researched, namely (i) breathing simulation, (ii) patient-ventilator interaction testing and (iii) aerosolised drug delivery. Measurement setups were developed allowing for each application to be tested and evaluated. This process, among other developments, included manufacturing of a physical model of the human upper respiratory tract and the integration of an optical aerosol spectrometer.

The main finding per application is as follows. First, the breathing simulation has been shown to reliably capture flow and pressure changes for a range of tidal volumes and frequencies and to be representative of human breathing. The possibility of using polymer or organic-based lung equivalents is unique and allows for the representation of processes naturally occurring during the human respiration cycle. Second, a new approach to testing patient-ventilator interactions has been introduced. The results show that different asynchronies can be triggered when the simulator is used to represent a patient undergoing assisted mechanical ventilation. Third, the number concentration and size distribution of aerosol particles generated by commonly used dry powder inhalers can be experimentally evaluated during simulations of inhalation and exhalation. This approach proposes an alternative to animal experimentation suitable for applications in aerosol research.

The thesis contains original research that has been presented at international conferences and published in three impact factor journals. The results of this thesis enable further teaching and research activities in respiratory research.